GENOMIC INSIGHTS OF AN ANDEAN MULTI-RESISTANT SOIL ACTINOBACTERIUM OF BIOTECHNOLOGICAL INTEREST

Daniel Alonso-Reyes[1]; Fátima Silvina Galván[1], Luciano Raúl Portero[1]; Natalia Noelia Alvarado[1]; María Eugenia Farías[2]; Martín P. Vazquez[3]; Virginia Helena Albarracín[1,4]*

[1]Laboratorio de Microbiología Ultraestructural y Molecular, Centro Integral de Microscopía Electrónica (CIME), Facultad de Agronomía y Zootecnia, UNT y CONICET, Tucumán, Argentina

[2]Laboratorio de Investigaciones Microbiológicas de Lagunas Andinas (LIMLA), Planta Piloto de Procesos Industriales y Microbiológicos (PROIMI), CCT, CONICET, Tucumán, Argentina.

[3]HERITAS-CONICET, Ocampo 210 bis, Predio CCT, Rosario, 2000, Santa Fe.

[4]Facultad de Ciencias Naturales e Instituto Miguel Lillo, Universidad Nacional de Tucumán, Tucumán, Argentina.

Running headline: ANDEAN MULTI-RESISTANT SOIL ACTINOBACTERIUM

Keywords: NESTERENKONIA, SOIL, PUNA, GENOMICS, EXTREMOPHILES, BIOTECHNOLOGY

*Corresponding author:

Virginia Helena Albarracín, Centro Integral de Microscopía Electrónica (CIME, CONICET, UNT) Camino de Sirga s/n. FAZ, Finca El Manantial, Yerba Buena (4107). Tucumán, Argentina. E-mail: cime@tucuman-conicet.gov.ar

HIGHLIGHTS

- Arid Andean Soils are attractive sources of microbial strains useful in biotechnological processes.
- Physiological studies revealed the multi-resistant nature of the poly-extremophile *Nesterenkonia sp.* Act20.
- Act20's genome analysis showed a complete set of genes coding for proteins involved in resistance to multiple stresses, including extremoenzymes and extremolytes.

ABSTRACT

Central Andean Ecosystems (between 2000 and 6000 masl) are typical arid to semiarid environments suffering from the highest total solar and UVB radiation on the planet but displaying numerous salt flats and shallow lakes. Isolated from these environments, Andean Microbial Communities (AME) of exceptional biodiversity endures multiple severe conditions. Also, the poly-extremophilic nature of AME's microbes indicates the potential for biotechnological applications. In this context, the presented study used genome mining and physiological characterization to reveal the multi-resistant profile of *Nesterenkonia sp.* Act20, an actinobacterium isolated from the soil surrounding Lake Socompa, Salta, Argentina (3570 m). UV-B, desiccation, and copper assays showed the strain's exceptional resistance to all these factors. Act20's genome presented coding sequences involving antibiotics, low temperatures, UV and arsenic resistance, nutrient limiting conditions, osmotic stress response, low atmospheric oxygen pressure, heavy metal stress, and resistance to fluoride and chlorite. Act20 can also synthesize proteins and natural products such as an insecticide, bacterial cellulose, ectoine, bacterial hemoglobin, and even antibiotics like colicin V and aurachin C. We also found numerous enzymes for animal and vegetal biomass degradation and application in other industrial processes .

The herein report shed light on the microbial adaptation to high-altitude environments, its possible extrapolation for studying other extreme environments of relevance, and its application to industrial and biotechnological processes.

INTRODUCTION

Central Andean Ecosystems (between 2000 and 6000 masl) are typical arid to semiarid environments suffering from the highest total solar and UVB radiation on the planet, displaying numerous salt flats and shallow lakes (Albarracín et al., 2016, 2015). Spanning from the Atacama Desert in Chile, through the Argentinean and Bolivian Puna up to the Peruvian Andes, these ecosystems experience a wide daily temperature range, high salinity (up to 30%), scarce nutrient availability and high concentration of heavy metals and metalloids, especially arsenic (Albarracín et al., 2016, 2015).

Despite these conditions, Andean Microbial Communities (AME) prove exceptional biodiversity and diverse strategies for enduring these severe conditions (Albarracín et al., 2016, 2015; Solon et al., 2018). Likewise, the importance of exploiting AME poly-extremophiles' full potential in terms of their biotechnological applications was highlighted (Albarracı and Farías, 2012). Examples are the production of waxes and fatty acids for biodiesel (Bequer Urbano et al., 2013) or compatible solutes, antioxidants, pigments, or enzymes for the pharmaceutical industry (Farias et al., 2011). Current projects heading this way have yielded detailed molecular information and functional proof on novel extremoenzymes: i.e., photolyase of *Acinetobacter sp.* Ver3 (Albarracín et al., 2014), an arsenical resistance efflux pump, and a green tuned microbial rhodopsin (Albarracin et al., 2015) in *Exiguobacterium sp.* S17 (Ordoñez et al., 2015).

Actinobacteria are high GC (50-71 %), Gram-positive microbes found in both terrestrial and aquatic ecosystems (Albarracín et al., 2005; Montalvo et al., 2005). Being the soil microbiota's main component (Schrempf, 2013), Actinobacteria exhibit various morphologies (Ventura et al., 2007), physiological and metabolic properties, and includes many species, which are useful in biotechnology (Kurtböke, 2003). Previous

work using dependent and independent culture techniques revealed that *Actinobacteria* is one of the predominant taxonomical groups among the AME's microbial communities (Dib et al., 2008, 2009; Rasuk et al., 2017). Moreover, AME's *Actinobacteria* have been demonstrated to carry giant linear plasmids that may involve the community's spread of resistance traits (Dib et al., 2010). AME's actinobacteria also showed their potential for producing secondary metabolites useful for the pharmacy industry. Wichner et al. (2017) reported that the extremotolerant isolate, *Lentzea* sp H45, synthesized new monoene, and diene glycosides. These natural products called lentzeosides A-F possess inhibitory activity against HIV integrase, a key enzyme for recombining the HIV genome into the host genome. Schulz et al. (2011) evidenced the production of bioactive compounds called abenquines (simple aminobenzoquinones substituted by different amino acids) by *Streptomyces* sp. DB634. Abenquines showed moderate inhibitory activity against phosphodiesterase type 4 (PDE4b) while proved useful for treating inflammatory diseases. Moreover, *Streptomyces* C38 produces 22-membered macrolactonic antibiotics atacamycin A-C, also considered drugs for treating inflammatory diseases by inhibiting PDE4b and antitumor by acting against tumor cell lines (Nachtigall et al., 2011).

Nesterenkonia is a particular genus (Stackebrandt et al., 1995) with most representatives isolated from hypersaline or alkaline environments such as saline soil, solar salt, seafood, soda lake, or alkaline wastewater. Halophiles are exploitable microorganisms for bioprocesses (Fu et al., 2014; Liu et al., 2019; Yin et al., 2014) (Yue et al., 2014). For example, *Nesterenkonia MSA 31* isolated from a marine sponge *Fasciospongia cavernosa* produces a halo-alkali and thermal tolerant biosurfactant useful as an emulsifier stabilizing agent in the food industry (Kiran et al., 2017). Furthermore, *Nesterenkonia* sp. strain F isolated from Aran-Bidgol Lake (Iran) can

produce acetone, butanol, ethanol, acetic, and butyric acids under aerobic and anaerobic conditions (Amiri et al., 2016). Also, *Nesterenkonia lacusekhoensis EMLA3* degrades reactive violet 1 (RV1), a toxic azo dye, under conditions of high pH and in the presence of a high concentration of NaCl, both of which generally inhibit microbial treatment process (Prabhakar et al., 2019). Thus, *Nesterenkonia* strains are attractive microbes in the search for biotechnological resources.

In a previous screening for extremophilic *Actinobacteria* from Puna arid alkaline soil, the dark yellow-pigmented *Nesterenkonia sp.* Act20 strain was identified (Rasuk et al., 2017). Act20 grew at a high concentration of NaCl (25%), Na_2CO_3 (5mM), and arsenic (up to 200mM arsenate), in a wide range of pH 5-12, with optimal growth at alkaline pH (Rasuk et al., 2017). In subsequent works, our group evidenced that *Nesterenkonia* sp Act20 had a high tolerance to UV-B (up to 100 kJ/m^2) due to an integrated response to radiation called UV-resistome (Portero et al., 2019).

The following work aims to test the multi-resistance of the Act20 strain combining phenotypic profiling with in-depth genomic analysis. Also, we highlight the potential for biotechnological use of extremozymes and extremolytes coded in its genome.

1. MATERIALS AND METHODS

2.1. Strains and culture conditions. UV-resistant strain Act20 used in this study was previously isolated from soil around Lake Socompa (3,570 m) at the Andean Puna in Argentina (Albarracín et al., 2016, 2015) and belongs to the LIMLA-PROIMI Extremophilic Strain Collection. Bacterial strain *Nesterenkonia halotolerans* DSM 15474 belongs to DSMZ Bacterial Culture Collection, and we used it as a control following previously reported works (Rasuk et al., 2017). Both strains were grown in an

"H" medium (a medium modified for halophiles, containing NaCl 15 g L^{-1}, KCl 3 g L^{-1}, $MgSO_4$ 5 g L^{-1}, sodium citrate 3 g L^{-1}) added with 2% agar when applicable.

2.2. Multi-resistance assays. The resistance of strain Act20 cells to diverse physical and chemical stresses was tested when exposed to increasing concentrations of copper, high UV doses, and desiccation treatments. For studying the response to desiccation, cells were first grown aerobically at 30 °C overnight in a 10 ml nutrient broth medium on a rotary shaker. Cells were harvested, washed once with sterile NaCl solution (0.85 %, w/v), and resuspended to reach an OD_{600nm} of 2 (±0.1) in NaCl solution. Approximately 20 aliquots (100 µl each) from this cell suspension were spotted onto 0.45-µm filters (Sartorius, Göttingen, Germany). These filters were placed onto agar medium H plates and incubated at 30 °C for five days. The colonies were then let dry by incubation in empty sterile dishes at 25 °C and 18% of relative humidity for 50 days, and the viable count (CFU) was assessed at different times. The filters on which the strains were grown were added to sterile microcentrifuge tubes. The cells from each filter were resuspended separately, and the CFU was determined before and after desiccation treatment. The tolerance to desiccation was determined in Act20 and *N. halotolerans* DSM 15474 as control.

Resistance to UV irradiation and copper salts were tested by a quick qualitative method. For the copper resistance profile assays, aliquots of 5 µL of an overnight (OD_{600}≈0.6) culture were loaded onto H medium agar plates supplemented with 1, 2, or 3 mM $CuSO_4$. The control cultures consisted of an "H" medium without copper supplementation. Then they were incubated for 72 h at 30 ºC under continuous PAR luminosity conditions with an OSRAM 100 W lamp.

For the UV resistance assays, the cells were pre-culture on liquid medium H, and once at OD_{600nm} = 0,6 collected for serial dilutions. Aliquots of 5 µL were then loaded

onto medium agar plates and immediately exposed to UV-B irradiation (Vilbert Lourmat VL-4, the maximum intensity at 312 nm) 5 min (1,7 Kj m^{-2}), 15 min (5,1 Kj m^{-2}), and 30 min (10,4 Kj m^{-2}). Then they were incubated for 72 h at 30 ºC in the dark to prevent photoreactivation. UV-B irradiance was quantified with a radiometer (Vilbert Lourmat model VLX-3W) coupled with a UV-B sensor (Vilbert Lourmat model CX-312). The minimal intensity measured was 5,21 W m^{-2}, and maximal power was 5,4 W m^{-2}. Controls of unexposed samples were run simultaneously in the dark.

Microbial growth was recorded with tree signs (+++) when similar to the growth in controls, two signs (++) when it was slightly different from the growth in the controls, one sign (1 pts) when growth was low (isolated colonies), and no sign when it was no growth at all. Parallel assays were performed for *Nesterenkonia halotolerans* DSMZ 15474 to compare resistance profiles.

2.3. Microscopic observation and ultrastructural characterization of Act20 cells. These assays were designed to evaluate the morphology and ultrastructure of Act20 in challenging conditions similar to those present in their original environment, i.e., under high UV irradiation and chemical (copper) stress. The selected strains were grown in H medium at 30°C with shaking (180 rpm). Cells in the mid-log phase of growth were harvested by centrifugation (5000 rpm for 10 min). Pellets were washed twice in 0.9 % NaCl and were kept under starvation conditions for 18 h at 4 °C in the same solution. 20 ml of cell suspension was transferred to a sterile plate and were exposed to UV-B irradiation at different times, as indicated before. Copper-challenged cultures were likewise obtained by growing the cells in H medium with and without 3 mM Cu.

For scanning electron microscopy (SEM) and transmission electron microscopy (TEM), 100 µL aliquots were collected for each different treatment and centrifuged

(5,000 rpm for 10 min) to remove the supernatant. The pellets were immediately fixed with Karnovsky's fixative (a mixture of 2,66% paraformaldehyde and 1,66% glutaraldehyde) in a 0.1 M phosphate buffer pH 7.3, for 48 h at 4°C. For SEM, the cells were processed according to previously optimized methods (Zannier et al., 2019). Briefly, aliquots of 50 µl of samples fixed were placed in coverslips for electron microscopy and kept for three hours at room temperature. The samples were then dehydrated in graded ethanol (30%, 50%, 70%, 90%, and 100%) for 10 min each and finally maintained in acetone 100% for 40 min. The dehydration was completed with the critical drying point (Denton Vacuum model DCP-1), in which acetone was exchanged by liquid CO_2. Then, samples were mounted on stubs and covered by gold (Ion Sputter Marca JEOL model JFC-1100) and observed under a Zeiss Supra 55VP (Carl Zeiss NTS GmbH, Germany) scanning electron microscope belonging to the Electron Microscopy Core Facility (CIME). For TEM, the protocol from Albarracín et al. (2008) was followed. After fixation, samples were washed twice in 0.1 M phosphate buffer, pH 7.3 (5000 rpm for 10 min), and embedded in agar (Bozzola, 2007). Agar pellets were post-fixed in 1% osmium tetroxide in phosphate buffer, pH 7.3, overnight at 4°C. After washing with the same buffer, and were stained in 2% uranyl acetate solution for 30 min at room temperature. The samples were dehydrated with ethanol solutions increasing concentrations (70%, 90%, and 100%) for 15 min each and finally maintained in acetone 100% for 30 min. After that, the infiltration and embedding in an acetone-SPURR resin sequence were carried out, followed by polymerization at 60°C for 24 h. Ultrathin sections were cut using a diamond knife on a manual ultramicrotome (Sorvall Porter-Blum Ultramicrotome MT-1). Bacteria were examined using a Zeiss LIBRA 120 (Carl Zeiss AG, Alemania) transmission electron microscope at 80 kV, belonging to the Electron Microscopy Core Facility (CIME-CONICET-UNT).

206 **2.4. Genome sequencing, assembly, and gap closure.** Genomic DNA from
207 *Nesterenkonia sp*. Act20 strain was purified from cells grown on LB broth for 72 h at
208 30° C and harvested by centrifugation (3,000 g for 10 min at 4◦C). Pellets were washed
209 twice with distilled water. We extracted total genomic DNA with the DNeasy Blood
210 and Tissue Kit (Qiagen) following the manufacturer's recommendations. Whole-genome
211 shotgun pyrosequencing was achieved using a 454 preparation kit (Roche Applied
212 Sciences, Indianapolis, IN, USA) and sequenced with a GS-FLX using Titanium
213 chemistry (454 Life Sciences, Roche Applied Sciences). The 454 reads were assembled
214 with Newbler Assembler software, v. 2.5.3, with –URT option. Extra-assembling
215 programs were run: MIRA v. 3.4.0 and Celera Assembler, v. 6.1. The different
216 assemblages were fused using MINIMUS 2 Pipeline from the AMOS Package. The
217 merged assembly was used as a guide for designing the primers, which were, in turn,
218 used to confirm contig joints and close gaps. The overall sequence coverage was 37X;
219 This Whole Genome Shotgun project has been deposited at DDBJ/ENA/GenBank under
220 the accession JADPQH000000000. The version described in this paper is version
221 JADPQH010000000.

222 **2.5. Genome analyses.** Genome annotation was implemented using PROKKA
223 (Seemann, 2014) with a custom expanded protein database, which includes Swiss-Prot,
224 TrEMBL, Pfam, SUPERFAMILY, TIGRFAM, and a genus-specific database built from
225 GenBank files downloaded from the NCBI database. We processed the set of annotated
226 FASTA files belonging to genomes with Proteinortho, which detects orthologous genes
227 within different species. For doing so, the software compares similarities of given gene
228 sequences and clusters them to find significant groups (Lechner et al., 2011).

229 **2.6. Phylogenetic analysis.** The sequence-based taxonomic analysis was performed
230 using both 16S rDNA and whole-genome comparisons. Sequences from genomes and

16S rDNA were obtained from the NCBI database (Assembly and RefSeq), and their characteristics resumed in Supplementary Table S1. Some 16S rDNA were retrieved from genome sequences to link both types of analysis. Sequences from 16S rDNA were aligned with Silva Incremental Aligner (Pruesse et al., 2012), and the phylogenetic tree was created with Fasttree 2.1.7 (Price et al., 2010) with the Maximum Likelihood method using Generalized Time-Reversible (GTR) model. Subsequent processing and visualization of the tree were performed with iTOL (Letunic and Bork, 2016). Genome-wide nucleotide identity trends were explored in the genome dataset by estimating all-against-all pairwise Average Nucleotide Identity (ANI). We utilized the ANIm approach that uses MUMmer (NUCmer) to align the input sequences as implemented in pyANI (Kurtz et al., 2004). The average between any given pair was used as the final value. Heat maps were generated using the heatmap V 1.0.12 R package (Kolde, 2019).

2. RESULTS

3.1. Taxonomic Affiliation of *Nesterenkonia* sp. Act20. *Nesterenkonia sp.* Act 20 was first isolated by Rasuk et al. (2017) and initially assigned to the genus by partial 16S rDNA sequencing. This work compared the full 16S rDNA sequence from Act20 with related strains, resulting in 98.2 % identity with *N. sandarakina* YIM 70009 and 97.4 % identity with both *N. jeotgali* JG-241 and N. *halotolerans* YIM70084. The phylogenetic tree based on this marker also suggests a close relationship of Act20 with the above mentioned plus *N. sp.* AN1, *N. aurantiaca* strains, *N. sandarakina*, and *N. Lutea*, clustering together in a significant clade (Fig. 1A). The whole-genome analysis using the ANI method shows a similar pattern of relationship (Fig. 1B). In this analysis, *N. sp.* Act 20, *N. aurantiaca* DSM 27373, *N. sp.* AN1, *N. jeotgali* CD087, and *N. sandarakina* CG 35 cluster with significance, and Act20 have a lower percent average nucleotide

256 difference (defined as 100% − ANI) value than the proposed 95% threshold (Richter
257 and Rosselló-Móra, 2009), suggesting that it could be a novel species.

258 **3.2. Multi-Resistance Profile of Act20.** Resistance to desiccation, UV, and copper was
259 uncovered in *Nesterenkonia* sp. Act20 and compared with the closest relative, *N.*
260 *halotolerans* (NH). A summary of this multi-resistance is presented in Table 1.
261 Tolerance to desiccation was tested every seven days for seven weeks. Act20
262 maintained its population in the same order of magnitude for 14 days, but from the third
263 week on, it showed null development (Fig. S1). In turn, NH decreased its population in
264 one order of magnitude after 7 and 14 days of treatment while it did not survive beyond
265 14 days of continuous drying conditions.

266 Tolerance to UV radiation was tested by placing culture serial dilutions drops of
267 the studied strains on "H" agar plates and exposing them to UV source as described
268 previously. A similar procedure was tried for testing resistance profiles to copper salts
269 in media amended with 1, 2, and 3 mM of copper. Our results showed that Act20 was
270 much more resistant to radiation than the selected control strain (Fig. S2), growing even
271 after a dose of 10,4 Kj m^{-2} of UV-B radiation. In turn, the copper resistance profile was
272 similarly high for both strains; Act20 and NH developed quite well even at the
273 maximum concentration tested (3 mM).

274 **3.3. General Genomic Features.** The assembly process led to two scaffolds: the largest
275 with 2,092,188 bp in length and G + C content of 65.98%, and the second scaffold with
276 836,993 bp and G + C content of 65.82%. As a whole, the genome of *Nesterenkonia* sp
277 Act20 consists of 2,930,097 bp, with a GC content of 65.9%. PROKKA annotation
278 shows 2,672 coding sequences, including 2,377 annotated genes and 58 RNAs. Act20
279 genomics features were compared to the other fifteen *Nesterenkonia* genomes available
280 in the NCBI assembly database (Table S7). Supplementary Table S2 shows the

281 annotated genes of Act20, their sequence length, and functions assigned by homology,
282 as well as the KO identifiers linked for some of these genes. A summary of the most
283 relevant annotated functions can be found in Supplementary Tables S3 and S4.

284 **3.4. Genome traits of Act20 multi-resistance phenotype.** Genome inspection
285 indicated genetic determinants coding for systems potentially involved in the high
286 resistance profile observed in herein described and previous lab assays (Rasuk et al.,
287 2017). The genome showed pathways associated with osmotic and oxidative stress
288 response, low temperature, starvation response, and low oxygen conditions,
289 unmistakable evidence of this microbe adaptation to its extreme and changing habitat. It
290 also has traits related to resistance to heavy metals (mainly copper and mercury),
291 antibiotics (mainly beta-lactams and vancomycin), arsenic, fluoride, and chlorite (Table
292 S3, S4).

293 Both, the Prokka and RAST annotations account for several genes for
294 resistance/tolerance to copper (Table 2). Among the direct mechanisms of resilience to
295 copper described by Giachino and Waldron (2020) in Act20 is worth to mention the *cop*
296 family, implicated in copper homeostasis through the capture and expulsion of Cu[I]
297 ions from the cytosol to the periplasm. This mechanism may be complemented by the
298 action of a copper oxidase necessary for converting Cu [I] to Cu [II], which is more
299 biologically inert and tend to remain in the periplasm. It is also interesting the presence
300 of a gene matching a recently discovered family of copper-binding proteins involved in
301 cytosolic copper storage (Dennison et al., 2018). On the other hand, the indirect
302 mechanisms would involve the participation of genes whose actions compensate for
303 specific damage caused by toxic copper. This is the case for the specific DsbD oxidase
304 which rearranges misfolded peptides, and the Fur master regulator of iron metabolism

that counteracts the constant scavenging of iron cofactors from enzymes, which in turn can generate ROS (Giachino and Waldron, 2020).

Previous assays carried out on Act20 revealed its ability to grow in alkaline media (up to pH 12) and at high NaCl (25%) and Na_2CO_3 (5 mM) concentrations (Rasuk et al., 2017). In this work, we also verify its desiccation tolerance, a phenotype that is supported by a vast repertory of genes (Table 3). This ability may be explained by the presence of transporters for the uptake of a diverse organic osmoprotectant such as glycine betaine, proline betaine, glycerol, choline, and trehalose. Genes for the synthesis of glycine betaine and the complete set of genes for ectoine were also detected (Table 3, Fig. S3). These compounds counteract the environment's high osmolality avoiding a rapid efflux of water from the cell and, consequently, the loss of turgor. Low turgor starts a rapid influx/synthesis of these osmo-protectants that complement another inorganic compounds (Lucht and Bremer, 1994; Nagata and Wang, 2001; Styrvold and Strom, 1991; Wood, 1988). Other genes, like OsmC and MdoB, are involved in coping the osmotic stress in peculiar ways (Atichartpongkul et al., 2001), specifically MdoB, whose product requires periplasm and outer membrane facilitate its effect (Sleator and Hill, 2002), both structures not normally present in Gram-positive bacteria including Act20.

The genomic profile of ABC transporters and the two-component system is also a reflection of the original environment. The set of proteins to sense phosphate limitation and subsequent phosphorus incorporation (in the form of phosphates and phosphonates) are evident (Fig. S4, S5). A similar is noticed for osmotic stress. Other environmental sensing types include oxygen limitation, low temperature, cell envelope stress, cell wall stress, and antibiotics. Transporters for iron and various organic

329 compounds such as carbohydrates (mostly of plant origin), nucleosides, amino acids,
330 and oligopeptides were also reported.

331 To discover unique functional traits of Act20, we searched the orthologous
332 sequences for public available *Nesterenkonia* genomes. The set of annotated FASTA
333 files belonging to genomes were processed through Proteinortho, which detect
334 orthologous genes within different species. The proteins of Act20 that did not match
335 any ortholog were analyzed one by one to verify if the annotated function they encode is
336 unique for Act20 and is not present in other representatives of the genera. Table 4
337 shows the exclusive traits of Act20, most of them related to its extreme natural
338 environments such as bacterial persistence, bacterial cell envelope stress response, and
339 resistance to osmotic stress, desiccation, and phosphate starvation. Degradative
340 enzymes 6-deoxy-6-sulfogluconolactonase and α-xylosidase take part in the
341 decomposition of prototrophic biomass present in the soil, from which Act20 could take
342 advantage. The remaining functions were characterized only at the protein domain level,
343 like ethyl tert-butyl ether degradation, second messenger's sensors, and cell wall
344 binding.

345 **3.5. UV-Resistome of Act20.** The high UV-resistance profile of Act20 calls for more
346 in-depth characterization and points out the existence of integrated physiological and
347 molecular mechanisms triggered by ultraviolet light exposure. We named this system
348 "UV-resistome" as described before for other AME poly-extremophiles (Kurth et al.,
349 2015; Portero et al., 2019). Ideally, the UV-resistome depends on expressing a diverse
350 set of genes devoted to evading or repairing the damage provoked directly or indirectly.
351 Ideally, it encompasses the following subsystems: (1) UV sensing and effective
352 response regulators; (2) avoidance and shielding strategies; (3) damage tolerance and
353 oxidative stress response; and (4) DNA damage repair. Therefore, we screened genes

associated with each of these UV-B resistome subsystems for all available genomes of the *Nesterenkonia* genus. This approach unveiled the relative genomic potential of Act20 to defend itself from UV-B radiation, a strain that naturally endures the highest irradiation on the planet. Unlike previous works, we studied the UV-resistance integrally and included genes that could have the potential to generate a UV evasion response or could lessen the negative impact the light, such as motility genes, pilus, and gas vesicles (Damerval et al., 1991).

Table S5 details the UV-resistome for every strain and clusters it by subsystems. The collections summarized all types of damage repair (base excision repair, nucleotide excision repair, mismatch repair, homologous repair, direct repair, homologous repair, direct repair, translesion DNA synthesis factors, and SOS response factors) explicitly, oxidative stress response and UV avoidance/protection mechanisms (synthesis of photoprotective pigments, and genes for flagellum, pilus, gas vesicles, and swarming motility; Fig. 2). The bars are sorted from top to bottom, taking into account the number of different genes for each subsystem. Act20 is positioned at the top with the most diverse and complete UV-resistome, with 114 genes, followed by NBAIMH1 with 107 genes, which also belongs to an extreme altitude environment. Interestingly, other strains from harsh environments with expected high solar radiation, such as AN1 and M8 with 85 and 83 genes, respectively, also have robust UV-resistomes. On the other hand, strains belonging to environments with little or null exposure to solar radiation present less diverse and fewer genes: i.e., *N. alba*. DSM19423, GY074, and RB2 with 56, 63, and 65 genes, respectively.

3.5. Ultrastructural changes in UV-challenged Act20 cells. The morphology and ultrastructure of the actinobacterium *Nesterenkonia* sp. Act20 was observed under UV challenging and non-challenging conditions to determine their behavior in their original

379 environment. *Nesterenkonia halotolerans* DSM 15474 (NH) was used for comparison.
380 Under SEM, in normal conditions, Act20 and DSM 15474 cells appear as irregular
381 coccoids or short rod-shaped. Their size varied between 0.41-0.43 x 0.6-0.82 µm for
382 Act20 and 0.41-0.38 x 0.71-0.51 for NH. The surface was smooth without evidence of
383 cell wall rupture (Fig. 3A, 3E). In contrast, after exposure to UV both strains exhibited
384 morphological alterations, which were consistently more severe in NH cells.

385 As the dose increases, Act20 morphology changed as individuals became
386 longer and sometimes wide, probably due to cell division's interruption, causing a
387 complete deformation in the cell (see black arrows in Fig. 3C, 3D). Furthermore, the
388 cells' surface appeared with shrinkage signs (see white arrows in Fig. 3C). In NH,
389 fibrilar structures were observed only on the surface of cells treated for 5 and 15 min
390 with RUV (Fig. 3F, 3G). We found that at the dose of 0,51 Jls/cm2 (15 min), the pili
391 thickened, and in some sections, they broke or disintegrated (see Fig. 3G, white arrows).
392 At 30 min of exposure (Fig. 3H), cell aggregates were observed in which bacterial cells
393 adhered to one another by self-produced extracellular polymeric (EPS) substances. The
394 surface irregularity was also found, indicating the wall cell rupture and degradation,
395 probably causing cell lysis (Fig. 3H, black arrow).

396 TEM images for both strains were likewise obtained (Fig. 4). EM analysis
397 revealed the typical Gram-positive bacteria structure, an intense electron opaque inner
398 layer corresponding to the cytoplasmic membrane (CM) and a less electron opaque
399 outer layer or cell wall (CW).

400 Ultrastructural changes were observed in the cells after exposure to UV
401 radiation, especially at the structural membrane level, acquiring a certain degree of
402 disorganization compared to the untreated strains (controls). A general observation in

403 both UV-treated bacteria was that numerous cells contained septa (S), compared to
404 control samples. Radiation stress probably caused the cell division process to stop at
405 this point without completing cell separation, whereas in control cells, the division was
406 normal.

407 Furthermore, variations in the cell envelope thickness were frequently observed
408 (see black arrows in Fig. 4). During the highest doses of UVR (15 and 30 min
409 exposure), the different cytoplasmic structures were visualized by electron density
410 variations. In Act20, polyphosphate-like granules (G) were visible, appearing as
411 electron-dense aggregates, scattered throughout the cytoplasm but surrounding the
412 nucleoid (N), with diameters varying between 0.2-0.3 μm (Fig. 4C, 4D); as well as
413 mesosome-like structures (m) formed from projections of the cytoplasmic membrane
414 (Fig. 4D). Also, the interaction between neighboring cells could be observed (see white
415 arrows in Fig. 4D). In NH, the damage caused by UV at the cytoplasmic membrane
416 level was more pronounced. The heterogeneous and disorderly appearance (see grey
417 arrows in Fig. 4G, 4H) could result from loss of membrane integrity, leading to a
418 malfunction of the permeability barrier and inducing cell lysis. Mesosome-like
419 structures (m) (Fig. 4G, 4H) are frequent, and the interaction between bacteria mediated
420 for pili or EPS is a common feature too (see white arrows).

421 **3.5. Genome insights in Act20 biotechnological potential.** Act20 is a halophile with
422 enormous biotechnological potential, as it encodes haloenzymes and proteins with
423 current applications in the food industry, waste treatment, medicine, cosmetics,
424 biocontrol, pharmacology, paper industry, bioremediation, fuel, and chemical industry
425 (Table 5).

426 Act20 could degrade wasted vegetal biomass, especially lignocellulose
427 derivatives, as it encodes α-xylosidase, xylanases, xylose isomerases, and an α-

arabinofuranosidase. Also has a chitinase, which confers the potential to degrade wasted animal biomass. The genome of Act20 also reports the possibility of producing some exciting compounds of interest; these include bacterial cellulose, a compound with an emerging number of applications such as nanoparticle science and regenerative medicine (Gullo et al., 2018); bacterial hemoglobin, which was previously showed to enhance bioproduction upon low oxygen conditions (Frey and Kallio, 2003), promising antibiotics like colicin and aurachin (Gérard et al., 2005; Gerhard Hofle et al., 1987; Mousa et al., 2016; Oettmeier et al., 1994), and the protein Cry26Aa with high insecticide properties (Wojciechowska et al., 1999). Another relevant enzyme provided by the Act20 genome is the α-sialidase, which has been proven to be useful in synthesizing sialylated glycoproteins (Kim et al., 2011) highly suitable for pharmacology (Varki, 2008).

3. DISCUSSION

Nesterenkonia sp. Act20 is an actinobacterium isolated from an Andean soil in the Puna region, one of the most extreme environments on the planet, which even NASA has used to test microbes and equipment for spatial explorations (Cabrol et al., 2007; Cockell et al., 2019). Although the polyextremophilic nature of Act20 was preliminary explored before, its genome's functional characteristics have remained uncovered. In this work, we revealed the genomic basis of the multi-resistance phenotype of strain Act20, especially towards UV radiation, copper and desiccation. Its potential on the production of enzymes and compounds useful for biotechnology was likewise explored.

The 'extreme' environmental conditions suffered in its original environment –arid soil at 3,600 m- challenged Act20 to evolve mechanisms to tolerate a wide range

453 of chemical and physical stresses. They include strong fluctuations in daily temperature,
454 hypersalinity, alkaline pH, high levels of UV radiation, a low nutrient availability,
455 desiccation, and high concentrations of heavy metals and metalloids, especially arsenic
456 (Albarracín et al., 2016, 2015; Dib et al., 2008, 2009; Farías et al., 2009; Fernández
457 Zenoff et al., 2006; Ordoñez et al., 2009). *Nesterenkonia* strains were frequently
458 isolated from environmental niches, including other saline locations (Amiri et al., 2016;
459 Yoon et al., 2006). It was demonstrated that the ecology of these diverse habitats
460 defines the genetic differentiation of *Nesterenkonia*. Such genetic differentiation seems
461 to be a key feature in the genome of Act20 as it shares low sequence similarity with
462 other strains of the set of genomes analyzed with ANI. The genomic and physiological
463 particularities suggests Act20 may be a new species adapted to the HAAL environment;
464 experiments heading this way are currently in progress in our lab (Fig. 1).

465 Act20´s copper and desiccation resistance described before is coincident
466 with several sequences found it its genome potentially involved in such resistance. It is
467 noteworthy the abundance of direct and indirect mechanisms implicated in the copper
468 resistance; some of them were well studied in Gram-negative bacteria and are
469 performed by periplasmic proteins, which are unlike to exist the Gram-positive Act20
470 which lacks outer membrane and periplasm (Giachino and Waldron, 2020). Likewise,
471 the desiccation resistance relies on the production of a wide diversity of
472 osmoprotectants that creates a hydrostatic force in the cytoplasm; the puzzling fact is
473 that MdoB protein would provoke such hydrostatic pressure only in the periplasm. In
474 both cases, it will be interesting to assess whether Act20 cell wall structure can
475 accommodate a periplasmic-like space where the described gene products can function
476 as proposed for Gram-negative bacteria, periplasmic space was reported for other Gram-
477 positive bacteria (Matias and Beveridge, 2005; Zuber et al., 2006).

A particular cytosolic copper storage protein in the annotation analysis called our attention. Its function and existence are controversial since a widely accepted view is that bacteria have not evolved to use intracelullar copper accumulation due to potential toxicity associated with their metalation (Dennison et al., 2018). Note that this protein was initially discovered in the Gram-negative methane-oxidizing bacterium (methanotroph) *Methylosinus trichosporium* OB3b, which use large amounts of copper to metabolize methane via the membrane-bound (particulate) methane monooxygenase (pMMO) (Vita et al., 2015). Nevertheless, it is not clear the role of this copper storage in Act20 which can otherwise work as an additional osmoprotectant. More research will be needed to confirm the copper bioaccumation ability of Act20, a mechanism useful for the design of bioremediation processes and applicable to several pollutant activities such as industry and mining.

The complete set of genes for ectoine synthetic cluster is present in Act20 genome (Fig. S3), conferring the strain an excellent potential for future biotechnological applications. Ectoine is a water-binding zwitterionic amino acid derivative with numerous biotechnological applications. It is a common component of cosmetic anti-aging and moisturizing creams to improve skin resistance to surfactants in skin cleansing solutions. It also alleviates skin inflammation, being currently recommended to treat moderate atopic dermatitis (Bownik and St□pniewska, 2016). Furthermore, the compound is useful in sunscreens as it strongly absorbs ultraviolet (UV) radiation and protects DNA from breaking down in diverse cell types. Ectoine also has applications in medicine: it can inhibit HIV replication and stabilize retroviral vectors for gene therapy (Bownik and St□pniewska, 2016). The alleviation of certain kinds of inflammation (colitis and neutrophilic lung inflammation) and allergic rhinitis were also reported,

even preventing the amyloid formation and delaying the onset and progression of Alzheimer's disease (Bownik and St□pniewska, 2016).

Metabolism of arsenic, a toxic element that can limit or suppress bacterial growth, is also possible for Act20. It has previously been demonstrated that Act20 can tolerate arsenic in the form of As (V) (0-200 mM) (Rasuk et al., 2017). In this work, we reported the presence of an arsenate reductase (not specified), an arsenate-mycothiol transferase, an arsenic transporter (not specified), and seven regulators of the ArsR family (Table S3). We propose that this resistance probably occurs by reducing As (V) to As (III) with a mycothiol-dependent arsenate reductase and subsequent efflux of As (III) from the cell using specific transporters (Ordóñez et al., 2009). Thus, the genome of Act20 joins others already sequenced from HAAL extremophilic prokaryotes (Burguener et al., 2014; Farias et al., 2011; Ordoñez et al., 2015, 2013), being the first of the *Nesterenkonia* genus reported for an environment with a high concentration of arsenic, and the first HAAL genome reporting the reduction of As (V) to As (III) through the mycothiol/thioredoxin redox pathway.

The genome of Act20 also seems to be optimized to cope with low nutrient availability, particularly phosphorous, as genes for a phosphorous-specific two-component system and transporters are well represented (Fig. S4, S5). The two-component system detects low phosphorous availability and communicates the signal to the cell, which expresses phosphate and phosphonate active transporters. Also, two phosphate starvation inducible proteins were reported in the annotation, PhoH, and SphX (Table 4, Table S3), being the latter unique of Act20 and no present in other *Nesterenkonia*. The genomic data also reveals that Act20 could face carbon starvation as its genome codifies active transporters to uptake several kinds of peptides, nucleotides, amino acids, and carbohydrates from the environment (Table S3, Fig. S4).

Nesterenkonia sp. Act20 genome is the first one of this genus reported from the highest UV irradiation environment on Earth: Puna-High Andes region; in accordance, we found genetic traces for complex UV resistance mechanisms comprehensively called as UV-resistome. The comparison of UV-genomic determinants of Act20 with other *Nesterenkonia* genomes indicated indeed a more sophisticated UV-resistome for the Socompa strain. It is then evident that environmental irradiation has a notable impact on the genome of Act20, which has a higher quantity and diversity of genes dedicated to UV resistance than other strains less irradiated. We also observed a similar pattern for other *Nesterenkonia* from high altitude or expected high irradiated environments (Fig. 2, Table S7). Interestingly, solar irradiation intensity selecting UV-resistome gene abundance and diversity in aquatic microbiomes was also evidenced by our group using a worldwide metagenomic analysis (Alonso-Reyes et al., 2020).

Among the subsystem of UV evasion/shielding is worth to note the genes involved in the production of gas vesicles (gvpA, K, O and F). Certainly, the expression of gas vesicles (Damerval et al., 1991; Englert et al., 1992; Pfeifer, 2012) along with flagella, allow microbes to move up in the water column toward sunlight. However, in many cases, these vesicles are also present in soil prokaryotes, even from high UV radiation environments, thus suggesting new roles in radiation protection (Oren, 2012). It has been speculated that they could change the cell position concerning the angle of the light's incidence, changing its impact on the cell (Bolhuis et al., 2006; Oren, 2012). Additionally, our current works on comparative proteomics reveal an increase in vesicle proteins' expression in response to the UV increase (Zannier et al., in preparation). We also include flagella, swarming motility proteins and the pili, whose ability to promote bacterial aggregation or biofilm adhesion may protect the cells from the UV exposure (Burdman et al., 2011; Ojanen-Reuhs et al., 1997).

552 Act20 genome codes resistance genes to other extreme factors: low
553 temperatures, low atmospheric O_2 pressure, heavy metal and other toxic compounds
554 stress. Many of these hard environmental factors added to the previously mentioned and
555 geophysical characteristics of the sampling site resembles those present in Early´s Earth
556 atmosphere that witnessed the evolution of ancient microorganisms (Albarracín et al.,
557 2015; Cabrol et al., 2007) (Fig. 5) (Cockell et al., 2000; Forni et al., 2015; Hecht et al.,
558 2009; Karunatillake et al., 2007; Sforna et al., 2014; Wadsworth and Cockell, 2017;
559 Yen et al., 2006) (https://mars.nasa.gov/all-about-mars/facts/). Thus, Act20 is an
560 exciting model to study the mechanisms by which the extremophiles could have
561 successfully faced the adverse conditions of the Earth's history, having clear
562 implications on astrobiological projects (Hiscox and Thomas, 1995; Merino et al., 2019;
563 Slotnick, 2000).

564 Act20 could also have a great biotechnological potential for producing and
565 metabolizing compounds and enzymes of interest (Table 5). Bacterial cellulose,
566 hemoglobin, antibiotics, and a potential insecticide are among the Act20 biosynthetic
567 products. On the other hand, several genes for enzymes capable of degrade vegetal
568 biomass were also detected. This feature is of importance for the biodegradation of
569 lignocellulosic biomass of agro-industrial wastes which are produced in large amounts
570 through agricultural and forestry practices, including the paper-and-pulp and timber
571 industries. On the other hand, animal biomass that contains high proportions of
572 shellfish, such as shrimp, crab, and krill, are suitable to be processed through chitinases,
573 an enzyme that is also present in Act20. The seafood processing industry has raised
574 serious concerns regarding disposal issues because of this waste's low biodegradation
575 rate, which could be solved through an enzymatic approach.

The enzymes mentioned above could be used in industrial processes that reproduce the microbe's original natural habitat's extreme conditions. Biocatalysts isolated by these extremophiles are termed extremozymes and possess special salt allowance, thermostability, and cold adaptivity. Extremozymes are very resistant to severe conditions owing to their great versatility. As such, they represent new prospects for biocatalysis and biotransformations and the development of the economy and unique line of research through their application (Dumorné et al., 2017). Here, we also report the genetic potential of Act20 to provide poly-extremozymes, which could combine resistance to cold (-2 ° C - 20 ° C), high solar radiation, salinity (at least 1 M salt), and high pH (>8). Enzymes of this halophilic microbe could provide great opportunities, particularly for food, bioremediation, and pharmacy industries.

CONCLUSION

In this work, we have confirmed by lab assays the multi-resistance phenotype of *Nesterenkonia* sp. Act20, a poly-extremophile originally isolated from Puna arid soil surrounding Lake Socompa, in the Puna region, exposed to the highest irradiated environment on Earth. Accordingly, its genome codes for a plethora of genes that help counteract the ecological pressure of the hostile conditions face by the microbe in its original environment: i.e. arsenic, nutrient limiting conditions, osmotic stress, UV radiation, low temperatures, low atmospheric O2 pressure, heavy metal and other toxic elements stress.

As a novel extremophile, Act20 has the potential to produce compounds (extremolytes and extremoenzymes) of interest with application in industrial processes such as an insecticidal protein, bacterial cellulose, ectoine, colicin V, arauchins,

chitinases and cellulases. In this way, Act20 becomes an exciting candidate for additional studies of transcriptomics, proteomics (currently in progress), metabolomics, as well as the expression and testing of biotech-competent enzymes. The herein report shed light on the microbial adaptation to high-altitude environments, its possible extrapolation for studying other extreme environments of relevance, and its application to industrial and biotechnological processes.

4. ACKNOWLEDGEMENTS

The authors acknowledge the generous financial support by PIUNT G603 and PIP CONICET 0519 projects. VHA, MPV, and MEF are staff researchers from the National Research Council (CONICET) in Argentina. DA, MSG, NNA are the recipients of doctoral fellowships from CONICET. Act20 genome sequencing project was performed in INDEAR-CONICET, Argentina. Electron micrographs used in this study were taken at the Center for Electron Microscopy (CIME) belonging to UNT and CCT, CONICET, Tucuman. This manuscript has been released as a Pre-Print at bioRxiv.

REFERENCES

Albarracín, V., Simon, J., Pathak, G., … L.V.-P.&, 2014, U., 2014. First characterisation of a CPD-class I photolyase from a UV-resistant extremophile isolated from High-Altitude Andean Lakes. pubs.rsc.org.

Albarracín, V.H., Amoroso, M.J., Abate, C.M., 2005. Isolation and characterization of indigenous copper-resistant actinomycete strains. Geochemistry 65, 145–156. https://doi.org/https://doi.org/10.1016/j.chemer.2005.06.004

624 Albarracín, V.H., Gärtner, W., Farias, M.E., 2016. Forged Under the Sun: Life and Art
625 of Extremophiles from Andean Lakes. Photochem. Photobiol. 92, 14–28.
626 https://doi.org/10.1111/php.12555
627 Albarracín, V.H., Kurth, D., Ordoñez, O.F., Belfiore, C., Luccini, E., Salum, G.M.,
628 Piacentini, R.D., Farías, M.E., 2015. High-Up: A Remote Reservoir of Microbial
629 Extremophiles in Central Andean Wetlands. Front. Microbiol. 6, 1404.
630 https://doi.org/10.3389/fmicb.2015.01404
631 Albarracín, V.H., Winik, B., Kothe, E., Amoroso, M.J., Abate, C.M., 2008. Copper
632 bioaccumulation by the actinobacterium Amycolatopsis sp. AB0. J. Basic
633 Microbiol. 48, 323–330. https://doi.org/https://doi.org/10.1002/jobm.200700360
634 Albarracı, V.H., Farías, M.E., 2012. Biotecnología Turquesa. Rev. Hipótesis 13, 32–39.
635 Amiri, H., Azarbaijani, R., Parsa Yeganeh, L., Shahzadeh Fazeli, A., Tabatabaei, M.,
636 Hosseini Salekdeh, G., Karimi, K., 2016. Nesterenkonia sp. strain F, a halophilic
637 bacterium producing acetone, butanol and ethanol under aerobic conditions. Sci.
638 Rep. 6, 18408. https://doi.org/10.1038/srep18408
639 Bequer Urbano, S., Albarracín, V.H., Ordoñez, O.F., Farías, M.E., Alvarez, H.M., 2013.
640 Lipid storage in high-altitude Andean Lakes extremophiles and its mobilization
641 under stress conditions in Rhodococcus sp. A5, a UV-resistant actinobacterium.
642 Extremophiles 17, 217–227. https://doi.org/10.1007/s00792-012-0508-2
643 Bolhuis, H., Palm, P., Wende, A., Falb, M., Rampp, M., Rodriguez-Valera, F., Pfeiffer,
644 F., Oesterhelt, D., 2006. The genome of the square archaeon Haloquadratum
645 walsbyi : life at the limits of water activity. BMC Genomics 7, 169.
646 https://doi.org/10.1186/1471-2164-7-169
647 Bownik, A., St pniewska, Z., 2016. Ectoine as a promising protective agent in humans
648 and animals. Arh. Hig. Rada Toksikol. 67, 260–265. https://doi.org/10.1515/aiht-

649 2016-67-2837

650 Bozzola, J.J., 2007. Conventional specimen preparation techniques for scanning

651 electron microscopy of biological specimens. Methods Mol. Biol. 369, 449–466.

652 https://doi.org/10.1007/978-1-59745-294-6_22

653 Burdman, S., Bahar, O., Parker, J.K., de la Fuente, L., 2011. Involvement of type IV pili

654 in pathogenicity of plant pathogenic bacteria. Genes (Basel). 2, 706–735.

655 https://doi.org/10.3390/genes2040706

656 Burguener, G.F., Maldonado, M.J., Revale, S., Fernández Do Porto, D., Rascován, N.,

657 Vázquez, M., Farías, M.E., Marti, M.A., Turjanski, A.G., 2014. Draft Genome

658 Sequence of the Polyextremophilic Halorubrum sp. Strain AJ67, Isolated from

659 Hyperarsenic Lakes in the Argentinian Puna. Genome Announc. 2, e01096-13.

660 https://doi.org/10.1128/genomeA.01096-13

661 Cabrol, N.A., McKay, C.P., Grin, E.A., Kiss, K.T., Ács, E., Tóth, B., Grigorszky, I.,

662 Szabo, K., Fike, D.A., Hock, A.N., Demergasso, C., Escudero, L., Galleguillos, P.,

663 Chong, G., Grigsby, B.H., Román, J.Z., Tambley, C., 2007. Signatures of habitats

664 and life in Earth's high-altitude lakes: clues to Noachian aqueous environments on

665 Mars, in: The Geology of Mars Evidence from Earth-Based Analogs. pp. 349–370.

666 Cockell, C.S., Catling, D.C., Davis, W.L., Snook, K., Kepner, R.L., Lee, P., McKay,

667 C.P., 2000. The Ultraviolet Environment of Mars: Biological Implications Past,

668 Present, and Future. Icarus 146, 343–359.

669 https://doi.org/https://doi.org/10.1006/icar.2000.6393

670 Cockell, C.S., Harrison, J.P., Stevens, A.H., Payler, S.J., Hughes, S.S., Kobs

671 Nawotniak, S.E., Brady, A.L., Elphic, R.C., Haberle, C.W., Sehlke, A., Beaton,

672 K.H., Abercromby, A.F.J., Schwendner, P., Wadsworth, J., Landenmark, H., Cane,

673 R., Dickinson, A.W., Nicholson, N., Perera, L., Lim, D.S.S., 2019. A Low-

674 Diversity Microbiota Inhabits Extreme Terrestrial Basaltic Terrains and Their
675 Fumaroles: Implications for the Exploration of Mars. Astrobiology 19, 284–299.
676 https://doi.org/10.1089/ast.2018.1870
677 Damerval, T., Castets, A.-M., Houmard, J., de Marsac, N.T., 1991. Gas vesicle
678 synthesis in the cyanobacterium Pseudanabaena sp.: occurrence of a single
679 photoregulated gene. Mol. Microbiol. 5, 657–664. https://doi.org/10.1111/j.1365-
680 2958.1991.tb00737.x
681 Dennison, C., David, S., Lee, J., 2018. Bacterial copper storage proteins. J. Biol. Chem.
682 293, 4616–4627. https://doi.org/10.1074/jbc.TM117.000180
683 Dib, J., Motok, J., Zenoff, V.F., Ordoñez, O., Farías, M.E., 2008. Occurrence of
684 Resistance to Antibiotics, UV-B, and Arsenic in Bacteria Isolated from Extreme
685 Environments in High-Altitude (Above 4400 m) Andean Wetlands. Curr.
686 Microbiol. 56, 510–517. https://doi.org/10.1007/s00284-008-9103-2
687 Dib, J.R., Wagenknecht, M., Hill, R.T., Farías, M.E., Meinhardt, F., 2010. Novel linear
688 megaplasmid from Brevibacterium sp. isolated from extreme environment. J. Basic
689 Microbiol. 50, 280–284. https://doi.org/10.1002/jobm.200900332
690 Dib, J.R., Weiss, A., Neumann, A., Ordoñez, O., Estévez, M.C., Farías, E., 2009.
691 Isolation of Bacteria from Remote High Altitude Andean Lakes Able to Grow in
692 the Presence of Antibiotics *. Recent Pat. Antiinfect. Drug Discov. 1–11.
693 Dumorné, K., Córdova, D.C., Astorga-Eló, M., Renganathan, P., 2017. Extremozymes:
694 A potential source for industrial applications. J. Microbiol. Biotechnol. 27, 649–
695 659. https://doi.org/10.4014/jmb.1611.11006
696 Englert, C., Krüger, K., Offner, S., Pfeifer, F., 1992. Three different but related gene
697 clusters encoding gas vesicles in halophilic archaea. J. Mol. Biol. 227, 586–592.
698 https://doi.org/https://doi.org/10.1016/0022-2836(92)90914-6

699 Farías, M.E., Fernández-Zenoff, V., Flores, R., Ordóñez, O., Estévez, C., 2009. Impact
700 of solar radiation on bacterioplankton in Laguna Vilama, a hypersaline Andean
701 lake (4650 m). J. Geophys. Res. Biogeosciences 114.
702 https://doi.org/10.1029/2008JG000784
703 Farias, M.E., Revale, S., Mancini, E., Ordoñez, O., Turjanski, A., Cortez, N., Vazquez,
704 M.P., 2011. Genome sequence of Sphingomonas sp. S17 isolated from an alkaline,
705 hyperarsenic and hypersaline volcanic associated lake near 4000 meters above sea
706 level in the Argentinean Puna. J. Bacteriol. JB.05225-11.
707 https://doi.org/10.1128/JB.05225-11
708 Fernández Zenoff, V., Siñeriz, F., Farías, M.E., 2006. Diverse responses to UV-B
709 radiation and repair mechanisms of bacteria isolated from high-altitude aquatic
710 environments. Appl. Environ. Microbiol. 72, 7857–7863.
711 https://doi.org/10.1128/AEM.01333-06
712 Forni, O., Gaft, M., Toplis, M.J., Clegg, S.M., Maurice, S., Wiens, R.C., Mangold, N.,
713 Gasnault, O., Sautter, V., Le Mouélic, S., Meslin, P.-Y., Nachon, M., McInroy,
714 R.E., Ollila, A.M., Cousin, A., Bridges, J.C., Lanza, N.L., Dyar, M.D., 2015. First
715 detection of fluorine on Mars: Implications for Gale Crater's geochemistry.
716 Geophys. Res. Lett. 42, 1020–1028. https://doi.org/10.1002/2014GL062742
717 Frey, A.D., Kallio, P.T., 2003. Bacterial hemoglobins and flavohemoglobins: versatile
718 proteins and their impact on microbiology and biotechnology. FEMS Microbiol.
719 Rev. 27, 525–545. https://doi.org/10.1016/S0168-6445(03)00056-1
720 Fu, X.-Z., Tan, D., Aibaidula, G., Wu, Q., Chen, J.-C., Chen, G.-Q., 2014. Development
721 of Halomonas TD01 as a host for open production of chemicals. Metab. Eng. 23,
722 78–91. https://doi.org/https://doi.org/10.1016/j.ymben.2014.02.006
723 Gérard, F., Pradel, N., Wu, L.-F., 2005. Bactericidal Activity of Colicin V Is Mediated

by an Inner Membrane Protein, SdaC, of Escherichia coli. J. Bacteriol. 187, 1945 LP – 1950. https://doi.org/10.1128/JB.187.6.1945-1950.2005

Gerhard Hofle, B.K., Reichenbach, H., Hofle, G., 1987. The Aurachins, New Quinoline Antibiotics from Myxobacteria: Production, Physico-Chemical and Biological Properties. J. Antibiot. (Tokyo). 40, 258–265. https://doi.org/10.7164/antibiotics.40.258

Giachino, A., Waldron, K.J., 2020. Copper tolerance in bacteria requires the activation of multiple accessory pathways. Mol. Microbiol. 114, 377–390. https://doi.org/10.1111/mmi.14522

Gullo, M., La China, S., Falcone, P.M., Giudici, P., 2018. Biotechnological production of cellulose by acetic acid bacteria: current state and perspectives. Appl. Microbiol. Biotechnol. 102, 6885–6898. https://doi.org/10.1007/s00253-018-9164-5

Hecht, M.H., Kounaves, S.P., Quinn, R.C., West, S.J., Young, S.M.M., Ming, D.W., Catling, D.C., Clark, B.C., Boynton, W. V, Hoffman, J., DeFlores, L.P., Gospodinova, K., Kapit, J., Smith, P.H., 2009. Detection of Perchlorate and the Soluble Chemistry of Martian Soil at the Phoenix Lander Site. Science (80-.). 325, 64 LP – 67. https://doi.org/10.1126/science.1172466

Hiscox, J., Thomas, D., 1995. Genetic modification and selection of microorganisms for growth on Mars. J. Br. Interplanet. Soc. 48, 419–426.

Karunatillake, S., Keller, J.M., Squyres, S.W., Boynton, W. V, Brückner, J., Janes, D.M., Gasnault, O., Newsom, H.E., 2007. Chemical compositions at Mars landing sites subject to Mars Odyssey Gamma Ray Spectrometer constraints. J. Geophys. Res. Planets 112. https://doi.org/10.1029/2006JE002859

Kim, S., Oh, D.B., Kang, H.A., Kwon, O., 2011. Features and applications of bacterial sialidases. Appl. Microbiol. Biotechnol. 91, 1–15. https://doi.org/10.1007/s00253-

011-3307-2

Kiran, G.S., Priyadharsini, S., Sajayan, A., Priyadharsini, G.B., Poulose, N., Selvin, J., 2017. Production of Lipopeptide Biosurfactant by a Marine Nesterenkonia sp. and Its Application in Food Industry . Front. Microbiol. .

Kolde, R., 2019. R Package 'pheatmap.'

Kurtböke, D.I., 2003. Selective Isolation of Rare Actinomycetes. Queensland Complete Printing Services, Nambour, Queensland.

Kurth, D., Belfiore, C., Gorriti, M.F., Cortez, N., Farias, M.E., Albarracín, V.H., 2015. Genomic and proteomic evidences unravel the UV-resistome of the poly-extremophile Acinetobacter sp. Ver3. Front. Microbiol. 6, 1–18. https://doi.org/10.3389/fmicb.2015.00328

Kurtz, S., Phillippy, A., Delcher, A.L., Smoot, M., Shumway, M., Antonescu, C., Salzberg, S.L., 2004. Versatile and open software for comparing large genomes. Genome Biol. 5, R12. https://doi.org/10.1186/gb-2004-5-2-r12

Lechner, M., Findeiß, S., Steiner, L., Marz, M., Stadler, P.F., Prohaska, S.J., 2011. Proteinortho: Detection of (Co-)orthologs in large-scale analysis. BMC Bioinformatics 12, 124. https://doi.org/10.1186/1471-2105-12-124

Letunic, I., Bork, P., 2016. Interactive tree of life (iTOL) v3: an online tool for the display and annotation of phylogenetic and other trees. Nucleic Acids Res. 44, W242–W245. https://doi.org/10.1093/nar/gkw290

Liu, C., Baffoe, D.K., Zhan, Y., Zhang, M., Li, Y., Zhang, G., 2019. Halophile, an essential platform for bioproduction. J. Microbiol. Methods 166, 1–8. https://doi.org/10.1016/j.mimet.2019.105704

Lucht, J.M., Bremer, E., 1994. Adaptation of Escherichia coli to high osmolarity environments: Osmoregulation of the high-affinity glycine betaine transport

774 system ProU. FEMS Microbiol. Rev. 14, 3–20. https://doi.org/10.1111/j.1574-
775 6976.1994.tb00067.x
776 Matias, V.R.F., Beveridge, T.J., 2005. Cryo-electron microscopy reveals native
777 polymeric cell wall structure in Bacillus subtilis 168 and the existence of a
778 periplasmic space. Mol. Microbiol. 56, 240–251.
779 https://doi.org/https://doi.org/10.1111/j.1365-2958.2005.04535.x
780 Merino, N., Aronson, H.S., Bojanova, D.P., Feyhl-Buska, J., Wong, M.L., Zhang, S.,
781 Giovannelli, D., 2019. Living at the Extremes: Extremophiles and the Limits of
782 Life in a Planetary Context. Front. Microbiol. 10, 780.
783 https://doi.org/10.3389/fmicb.2019.00780
784 Montalvo, N.F., Mohamed, N.M., Enticknap, J.J., Hill, R.T., 2005. Novel actinobacteria
785 from marine sponges. Antonie Van Leeuwenhoek 87, 29–36.
786 https://doi.org/10.1007/s10482-004-6536-x
787 Mousa, W.K., Shearer, C., Limay-Rios, V., Ettinger, C.L., Eisen, J.A., Raizada, M.N.,
788 2016. Root-hair endophyte stacking in finger millet creates a physicochemical
789 barrier to trap the fungal pathogen Fusarium graminearum. Nat. Microbiol. 1,
790 16167. https://doi.org/10.1038/nmicrobiol.2016.167
791 Nachtigall, J., Kulik, A., Helaly, S., Bull, A.T., Goodfellow, M., Asenjo, J.A., Maier,
792 A., Wiese, J., Imhoff, J.F., Süssmuth, R.D., Fiedler, H.-P., 2011. Atacamycins A–
793 C, 22-membered antitumor macrolactones produced by Streptomyces sp. C38. J.
794 Antibiot. (Tokyo). 64, 775–780. https://doi.org/10.1038/ja.2011.96
795 Nagata, S., Wang, Y.B., 2001. Accumulation of ectoine in the halotolerant
796 Brevibacterium sp. JCM 6894. J. Biosci. Bioeng. 91, 288–293.
797 https://doi.org/https://doi.org/10.1016/S1389-1723(01)80136-5
798 Oettmeier, W., Masson, K., Soll, M., Reil, E., 1994. Acridones and quinolones as

799 inhibitors of ubiquinone functions in the mitochondrial respiratory chain. Biochem.
800 Soc. Trans. 22, 213–216. https://doi.org/10.1042/bst0220213
801 Ojanen-Reuhs, T., Kalkkinen, N., Westerlund-Wikström, B., Van Doorn, J., Haahtela,
802 K., Nurmiaho-Lassila, E.L., Wengelnik, K., Bonas, U., Korhonen, T.K., 1997.
803 Characterization of the fimA gene encoding bundle-forming fimbriae of the plant
804 pathogen Xanthomonas campestris pv. vesicatoria. J. Bacteriol. 179, 1280–1290.
805 https://doi.org/10.1128/jb.179.4.1280-1290.1997
806 Ordóñez, E., Van Belle, K., Roos, G., De Galan, S., Letek, M., Gil, J.A., Wyns, L.,
807 Mateos, L.M., Messens, J., 2009. Arsenate reductase, mycothiol, and mycoredoxin
808 concert thiol/disulfide exchange. J. Biol. Chem. 284, 15107–15116.
809 https://doi.org/10.1074/jbc.M900877200
810 Ordoñez, O., Lanzarotti, E., Kurth, D., Cortez, N., Farias, M., Turjanski, A., 2015.
811 Genome comparison of two Exiguobacterium strains from high altitude andean
812 lakes with different arsenic resistance: identification and 3D modeling of the Acr3
813 efflux pump . Front. Environ. Sci. .
814 Ordoñez, O.F., Flores, M.R., Dib, J.R., Paz, A., Farías, M.E., 2009. Extremophile
815 Culture Collection from Andean Lakes: Extreme Pristine Environments that Host a
816 Wide Diversity of Microorganisms with Tolerance to UV Radiation. Microb. Ecol.
817 58, 461–473. https://doi.org/10.1007/s00248-009-9527-7
818 Ordoñez, O.F., Lanzarotti, E., Kurth, D., Gorriti, M.F., Revale, S., Cortez, N., Vazquez,
819 M.P., Farías, M.E., Turjanski, A.G., 2013. Draft Genome Sequence of the
820 Polyextremophilic Exiguobacterium sp. Strain S17, Isolated from Hyperarsenic
821 Lakes in the Argentinian Puna. Genome Announc. 1, e00480-13.
822 https://doi.org/10.1128/genomeA.00480-13
823 Oren, A., 2012. The function of gas vesicles in halophilic archaea and bacteria: Theories

824 and experimental evidence. Life 3, 1–20. https://doi.org/10.3390/life3010001
825 Pfeifer, F., 2012. Distribution, formation and regulation of gas vesicles. Nat. Rev.
826 Microbiol. 10, 705–715. https://doi.org/10.1038/nrmicro2834
827 Portero, L.R., Alonso-Reyes, D.G., Zannier, F., Vazquez, M.P., Farías, M.E., Gärtner,
828 W., Albarracín, V.H., 2019. Photolyases and Cryptochromes in UV-resistant
829 Bacteria from High-altitude Andean Lakes. Photochem. Photobiol. 95, 315–330.
830 https://doi.org/10.1111/php.13061
831 Prabhakar, Y., Gupta, A., Kaushik, A., 2019. Enhanced decolorization of reactive violet
832 dye 1 by halo-alkaliphilic Nesterenkonia strain: Process optimization, short
833 acclimatization and reusability analysis in batch cycles. Process Saf. Environ. Prot.
834 131, 116–126. https://doi.org/https://doi.org/10.1016/j.psep.2019.09.004
835 Price, M.N., Dehal, P.S., Arkin, A.P., 2010. FastTree 2 – Approximately Maximum-
836 Likelihood Trees for Large Alignments. PLoS One 5, e9490.
837 Pruesse, E., Peplies, J., Glöckner, F.O., 2012. SINA: Accurate high-throughput multiple
838 sequence alignment of ribosomal RNA genes. Bioinformatics 28, 1823–1829.
839 https://doi.org/10.1093/bioinformatics/bts252
840 Rasuk, M.C., Ferrer, G.M., Kurth, D., Portero, L.R., Farías, M.E., Albarracín, V.H.,
841 2017. UV-Resistant Actinobacteria from High-Altitude Andean Lakes: Isolation,
842 Characterization and Antagonistic Activities. Photochem. Photobiol. 93, 865–880.
843 https://doi.org/10.1111/php.12759
844 Richter, M., Rosselló-Móra, R., 2009. Shifting the genomic gold standard for the
845 prokaryotic species definition. Proc. Natl. Acad. Sci. U. S. A. 106, 19126–31.
846 https://doi.org/10.1073/pnas.0906412106
847 Schrempf, H., 2013. Actinobacteria within soils: capacities for mutualism, symbiosis
848 and pathogenesis. FEMS Microbiol. Lett. 342, 77–78.

https://doi.org/10.1111/1574-6968.12147

Schulz, D., Beese, P., Ohlendorf, B., Erhard, A., Zinecker, H., Dorador, C., Imhoff, J.F., 2011. Abenquines A–D: aminoquinone derivatives produced by Streptomyces sp. strain DB634. J. Antibiot. (Tokyo). 64, 763–768. https://doi.org/10.1038/ja.2011.87

Seemann, T., 2014. Prokka: rapid prokaryotic genome annotation. Bioinformatics 30, 2068–2069. https://doi.org/10.1093/bioinformatics/btu153

Sforna, M.C., Philippot, P., Somogyi, A., van Zuilen, M.A., Medjoubi, K., Schoepp-Cothenet, B., Nitschke, W., Visscher, P.T., 2014. Evidence for arsenic metabolism and cycling by microorganisms 2.7 billion years ago. Nat. Geosci. 7, 811–815. https://doi.org/10.1038/ngeo2276

Sleator, R.D., Hill, C., 2002. Bacterial osmoadaptation: the role of osmolytes in bacterial stress and virulence. FEMS Microbiol. Rev. 26, 49–71. https://doi.org/10.1111/j.1574-6976.2002.tb00598.x

Slotnick, R.S., 2000. EXTREMOPHILIC TERRAFORMING. Am. Sci. 88, 124.

Solon, A.J., Vimercati, L., Darcy, J.L., Arán, P., Porazinska, D., Dorador, C., Farías, M.E., Schmidt, S.K., 2018. Microbial Communities of High-Elevation Fumaroles, Penitentes, and Dry Tephra “Soils” of the Puna de Atacama Volcanic Zone. Microb. Ecol. 76, 340–351. https://doi.org/10.1007/s00248-017-1129-1

Stackebrandt, E., Koch, C., Gvozdiak, O., Schumann, P., 1995. Taxonomic dissection of the genus Micrococcus: Kocuria gen. nov., Nesterenkonia gen. nov., Kytococcus gen. nov., Dermacoccus gen. nov., and Micrococcus cohn 1872 gen. emend. Int. J. Syst. Bacteriol. 45, 682–692. https://doi.org/10.1099/00207713-45-4-682

Styrvold, O.B., Strom, A.R., 1991. Synthesis, accumulation, and excretion of trehalose

874 in osmotically stressed Escherichia coli K-12 strains: Influence of amber
875 suppressors and function of the periplasmic trehalase. J. Bacteriol. 173, 1187–
876 1192. https://doi.org/10.1128/jb.173.3.1187-1192.1991
877 Varki, A., 2008. Sialic acids in human health and disease. Trends Mol. Med. 14, 351–
878 360. https://doi.org/10.1016/j.molmed.2008.06.002
879 Ventura, M., Canchaya, C., Tauch, A., Chandra, G., Fitzgerald, G.F., Chater, K.F., van
880 Sinderen, D., 2007. Genomics of Actinobacteria: tracing the evolutionary history
881 of an ancient phylum. Microbiol. Mol. Biol. Rev. 71, 495–548.
882 https://doi.org/10.1128/MMBR.00005-07
883 Vita, N., Platsaki, S., Baslé, A., Allen, S.J., Paterson, N.G., Crombie, A.T., Murrell,
884 J.C., Waldron, K.J., Dennison, C., 2015. A four-helix bundle stores copper for
885 methane oxidation. Nature 525, 140–143. https://doi.org/10.1038/nature14854
886 Wadsworth, J., Cockell, C.S., 2017. Perchlorates on Mars enhance the bacteriocidal
887 effects of UV light. Sci. Rep. 7, 4662. https://doi.org/10.1038/s41598-017-04910-3
888 Wichner, D., Idris, H., Houssen, W.E., McEwan, A.R., Bull, A.T., Asenjo, J.A.,
889 Goodfellow, M., Jaspars, M., Ebel, R., Rateb, M.E., 2017. Isolation and anti-HIV-1
890 integrase activity of lentzeosides A–F from extremotolerant lentzea sp. H45, a
891 strain isolated from a high-altitude Atacama Desert soil. J. Antibiot. (Tokyo). 70,
892 448–453. https://doi.org/10.1038/ja.2016.78
893 Wojciechowska, J.A., Lewitin, E., Revina, L.P., Zalunin, I.A., Chestukhina, G.G., 1999.
894 Two novel delta-endotoxin gene families cry26 and cry28 from Bacillus
895 thuringiensis ssp. finitimus. FEBS Lett. 453, 46–48.
896 https://doi.org/https://doi.org/10.1016/S0014-5793(99)00650-X
897 Wood, J.M., 1988. Proline porters effect the utilization of proline as nutrient or
898 osmoprotectant for bacteria. J. Membr. Biol. 106, 183–202.

https://doi.org/10.1007/BF01872157

Yen, A., Mittlefehldt, D., McLennan, S., Gellert, R., Bell, J., McSween, H., Ming, D., McCoy, T., Morris, R., Golombek, M.P., Economou, T., Madsen, M., Wdowiak, T., Clark, B., Jolliff, B., Schröder, C., Brückner, J., Zipfel, J., Squyres, S., 2006. Nickel on Mars: Constraints on meteoritic material at the surface. J. Geophys. Res. v.111 111. https://doi.org/10.1029/2006JE002797

Yin, J., Chen, J.-C., Wu, Q., Chen, G.-Q., 2014. Halophiles, coming stars for industrial biotechnology. Biotechnol. Adv. 33. https://doi.org/10.1016/j.biotechadv.2014.10.008

Yoon, J.H., Jung, S.Y., Kim, W., Nam, S.W., Oh, T.K., 2006. Nesterenkonia jeotgaki sp. nov., isolated from jeotgal, a traditional Korean fermented seafood. Int. J. Syst. Evol. Microbiol. 56, 2587–2592. https://doi.org/10.1099/ijs.0.64266-0

Yue, H., Ling, C., Yang, T., Chen, X., Chen, Y., Deng, H., Wu, Q., Chen, J., Chen, G.-Q., 2014. A seawater-based open and continuous process for polyhydroxyalkanoates production by recombinant Halomonas campaniensis LS21 grown in mixed substrates. Biotechnol. Biofuels 7, 108. https://doi.org/10.1186/1754-6834-7-108

Zuber, B., Haenni, M., Ribeiro, T., Minnig, K., Lopes, F., Moreillon, P., Dubochet, J., 2006. Granular layer in the periplasmic space of gram-positive bacteria and fine structures of Enterococcus gallinarum and Streptococcus gordonii septa revealed by cryo-electron microscopy of vitreous sections. J. Bacteriol. 188, 6652–6660. https://doi.org/10.1128/JB.00391-06

Figure and table legends

Figure 1. Phylogenetic analysis of *Nesterenkonia* strains. Strain *Nesterenkonia* sp. Act20 is in bold. (A) Maximum likelihood tree from the 16S rRNA gene. Black dots indicate that the gene was retrieved from a sequenced genome. (B) Heatmap based on whole-genome average nucleotide identity (ANI). *Act20* is distinct and inside the significant cluster.

Figure 2. The stacked bar chart shows the count of genes for all UV-resistome subcategories in colors, including the total count at the right end.

Figure 3. Scanning electron microscopy (SEM) micrographs of actinobacteria after exposure to UV-B radiation. **(A-D)** *Nesterenkonia* sp. Act20. **(E-H)** *Nesterenkonia halotolerans* DSM 15474. **(A, E)** Non-exposed growing bacterial cells (control). **(B, F)** Growing bacterial cells exposed to 0,17 Jls/cm2 of UV-B (5 min). **(C, G)** Growing bacterial cells exposed to 0,51 Jls/cm2 of UV-B (15 min). **(D, H)** Growing bacterial cells exposed to 1,04 Jls/cm2 of UV-B (30 min). Black arrows indicate changes morphological, and white arrows indicate damage in cells **(C)** and pili deterioration **(G)**. Scale bar 200 nm (E, F, G, H), 100 nm (A, B, C, D, E, F, H).

Figure 4. Transmission electron microscopy (TEM) micrographs of actinobacteria cells after exposure to UV-B radiation. **(A-D)** *Nesterenkonia sp.* Act20. **(E-H)** *Nesterenkonia halotolerans* DSM 15474. **(A, E)** Non-exposed growing bacterial cells (control). **(B, F)** Growing bacterial cells exposed to 0,17 Jls/cm2 of UV-B (5 min). **(C, G)** Growing bacterial cells exposed to 0,51 Jls/cm2 of UV-B (15 min). **(D, H)** Growing bacterial

947 cells exposed to 1,04 Jls/cm2 of UV-B (30 min). Scale bar 200 nm principal figure and
948 50 nm small box.

949 **Figure 5.** Comparison between the extreme conditions (relevant to Act20) of the Lake
950 Socompa, Mars surface, and the early Earth environments. The light brown box
951 represents the Act20 genome and its potential for the different resistances as described
952 inside.

953

954

955 **Table 1.** Multi resistance profile of Act20 strain and comparison with Nesterenkonia
956 halotolerans (NH)

957 **Table 2.** Group of genes potentially involved in the copper resistance reported for
958 Act20.

959 **Table 3.** Group of genes potentially involved in the desiccation resistance reported for
960 Act20.

961 **Table 4.** New functional traits (with no counterpart in other *Nesterenkonia*) of
962 *Nesterenkonia sp. Act 20* unveiled by genome functional annotation and ortholog
963 clustering.

964 **Table 5.** List of Act20's annotated enzymes and proteins with reported biotechnological
965 potential.

966 Tables

967 Table 1.

	Act20	NH
Desiccation Period		

7-days	+++	+
14-days	++	+
21-days	-	-

Copper Concentration		
1 mM	+++	+++
2 mM	++	++
3 mM	+	+

UV Dose		
1,7 Kj m^{-2}	+++	++
5.1 Kj m^{-2}	++	+
10.4 Kj m^{-2}	+	+

968

969

970 Table 2

Copper tolerance/resistance trait	**Function**
Copper-translocating P-type ATPase	Probably similar to P-type ATPase CopA, a secretes Cu(I) from the cytoplasm to the homeostasis (Giachino and Waldron, 2020).
CopC domain protein	CopC is a bacterial blue copper protein that molecule. Along with CopA, CopC mediates copper in the periplasm (Arnesano et al., 2003)

Putative CopD protein	Exact function not known. Involved in copper copper uptake in conjunction with CopC (Swiss
CopZ	Chaperone that serves for the intracellular sequ from the cytosol to the periplasm (Giachino and
Copper oxidase	Probably a periplasmic copper oxidase-like C the cytosol by converting periplasmic Cu(I) t inert, making it a relatively "safe" species for c Waldron, 2020).
DsbD domain-containing protein	DsbD (also known as CutA) oxidoreductase re incorrect disulfide bonds are inserted by toxic c
Four-helix bundle copper-binding protein	Cu(I) cytosolic storage. First found in meth amounts of copper to metabolize methane. Its what they are storing copper for remains unkno
Fur family ferric uptake transcriptional regulator	As toxic copper provokes mismetalation o regulator of iron metabolism is overexpressed copper resistance even at low copper concentra

971

972 Table 3.

Desiccation tolerance/resistance trait	Function
SugA-SugB-SugC	ABC transporter complex particular for the Involved in the recycling of extracellular containing molecules (Kalscheuer et al., 2010
Trehalase	Trehalose degradation. It may be nece

	intracellular trehalose (Carroll et al., 2007).
opuBC-OpuBB-OpuBA	High affinity multicomponent binding-prote osmoprotectant choline (Kappes et al., 1999)
ProX-ProW-ProV	ABC transporter complex involved in the betaine and proline betaine (Gul and Poolma
Choline dehydrogenase	Involved in the biosynthesis of the osmopr 1996).
Betaine-aldehyde dehydrogenase	Involved in the biosynthesis of the osmopro reversible oxidation of betaine aldehyde to 1997).
HTH-type transcriptional regulator BetI	Repressor involved in the biosynthesis of t represses transcription of the choline transp involved in the synthesis of glycine betaine (
EctA-EctB-EctC-EctD	Group of genes involved in the biosynth (Reshetnikov et al., 2006).
Glycerol uptake facilitator protein	Transporter of the osmoprotectant glycero (Hénin et al., 2008).
Phosphoglycerol transferase I MdoB	Participate in anionic polymers' biosynthe glucose units with an average charge of −5 potential across the outer membrane, resulti higher concentration in the periplasm than in to hydrostatic pressure in the periplasmic spa
OsmC	The osmotically inducible expression of the kind of role in the bacterial osmotic-stress res

974 Table 4.

Unique trait	Function
Protein SphX	High-affinity phosphate-binding protein induc and Gobler, 2013)
Serine/threonine-protein kinase toxin HipA	Toxin that induces bacterial persistence and 2013).
6-deoxy-6-sulfogluconolactonase	Sulfoquinovose degradation (Felux et al., 2015
Trehalase	Trehalose degradation (Carroll et al., 2007).
α-xylosidase	Catalyzes the liberation of alpha-xylose from t xyloglucan oligosaccharides (Matsuzawa et al.
4-deoxy-L-threo-5-hexosulose-uronate ketol-isomerase	Plays a role in the catabolism of hexuronat likely substituting for the regular hexuronat expression is repressed in these conditions (Ro
Pleckstrin homology domain (bPH_1)	Appears to be involved in the bacterial cell 2010).
SMODS-associated and fused to various effectors sensor (SAVED) domain	Senses nucleotide or nucleotide derivatives effectors deployed by a class of conflict syste sensing of the nucleotide second messengers (E
WxL domain	Cell wall binding in gram-positive bacte peptidoglycan (Brinster et al., 2007).
EthD domain	Related to the EthD protein, which is involved ether (ETBE) (Chauvaux et al., 2001)
Coronavirus endopeptidase C30	Involved in viral polyprotein processing in repl

975

976 Table 5.

Trait	Biotechnological applications
Alpha-xylosidase	Although a-xylosidases are relevant for th saccharides, only a few a-xylosidases have b unclear aspects regarding the properties of the (Matsuzawa et al., 2016). Before a-xylosida necessary to study its properties, and N. Act especially from the fact that N. Act 20 a-xylosic
1,4-beta-xylanases	Xylanases are used in the paper industry to i agents (hydrogen peroxide, ozone, chlorine) hemicellulose, reducing the amounts of blea process cost and increasing its eco-friendlin clarification of fruit juices and wines for impr the texture of bread. Furthermore, xylanases ar additives (Qeshmi et al., 2020).
Xylose isomerase	Usable in microbial cell factories or biorefiner fuels, chemicals, and other industrial derivates.
Chitinase (glycosyl hydrolase family 18)	Chitinases are suitable for 1) waste chitooligosaccharides and GlcNAc (which production of single-cell proteins for usage as post-harvest fungal pathogens, and 5) functiona used for example as a treatment for various fung
Exo-alpha-sialidase	Synthesis of sialylated glycoproteins. Sialic aci half-life of glycoproteins in circulation. Thus, i

	monosaccharides such as galactose are recogniz organs, and the glycoprotein is rapidly clea practical relevance for pharmacology beca (antibodies, cytokines, and hormones) are glyc 2008).
Alpha-L-arabinofuranosidase	Among the functions of microbial α-arabino Increase digestibility in the animal feed indu texture, and delay staling of bread, 3) increa industry, 4) serves in the clarification of juic reduce sugar content in bioethanol industry. production, antiglycemic agent production, sweetener production, and mycobacterial diseas
Cellulose synthase/poly-beta-1,6-N-acetylglucosamine synthase-like glycosyltransferase	These enzymes have critical roles in bacterial c malleable material that makes of it of enorm
Cellulose biosynthesis protein BcsQ	science, specially designing celluloses with ta properties. Native BC does not require any pur a number of biomedical applications. Adv
Cellulose synthase	regenerative medicine led to his usage in artifi hemostatic materials. One of the most exciting as wound healing scaffolds. BC is also appl Regarding to the cosmetic area, BC is extensiv as a powder in facial scrubs in association wit application in cosmetic is the production of co light transmittance, and permeability to liquid from BC can be used also in drug delivery for

	key role also in the food industry being used as beverages (due its ability to acquire flavors additive, it is used worldwide for its gelling hydrogel-like texture could be a new material Finally, BC is also applicable to bioremediati mercury and arsenic has been proved (Gullo et
Colicin V production protein	Colicin V (colV) is a secreted peptide antibio reducing competition for nutrients (Gérard e production of colV by an Enterobacter sp. stra Fusarium wilt in finger millet (Mousa et al., 201
Aurachin C monooxygenase/isomerase	This enzyme catalyzes the initial step in co Aurachins are quinoline alkaloids that act as a They have been reported to exhibit antimicr positive bacteria (Gerhard Hofle et al., 1987; O
Protein Cry26Aa	Promotes colloidosmotic lysis by binding to t having the potential to be used as a pesticidal (
Hemoglobin	Heterologous expression of bacterial hemoglo beneficial for mycelium forming microorganis Streptomyces strains, Acremonium crysogenur It is known that oxygen transfer to the myceli critical when such microorganisms are grown i such situations, BHb expression seems to enha improved the bioremediation capacity of Burk rate of 2,4-DNT degradation, where oxygen degradation pathway. Moreover, heterologous

	oxygen limitation in a wide range of distin productivity (Frey and Kallio, 2003).
Ornithine cyclodeaminase	Can be used for biotechnological production overexpressed in C. glutamicum (Jensen and W
Molybdate-binding protein ModA (Molybdate/tungstate-binding protein ModA)	It may be useful in radiopharmaceutical app bond-containing protein with increased affinity may be used to remove chromate, which is tox environmental aqueous solutions (Karpus et al.,

977

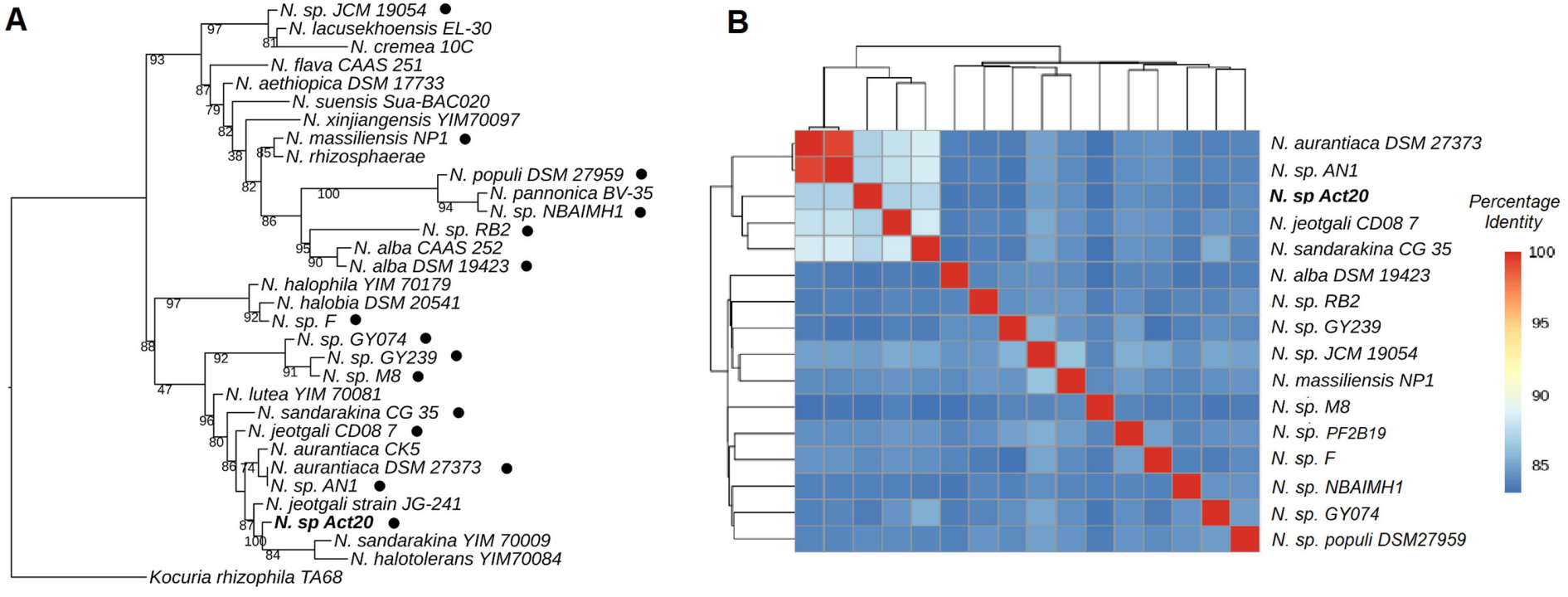
A
N. sp. JCM 19054
N. lacusekhoensis EL-30
N. cremea 10C
N. flava CAAS 251
N. aethiopica DSM 17733
N. suensis Sua-BAC020
N. xinjiangensis YIM70097
N. massiliensis NP1
N. rhizosphaerae
N. populi DSM 27959
N. pannonica BV-35
N. sp. NBAIMH1
N. sp. RB2
N. alba CAAS 252
N. alba DSM 19423
N. halophila YIM 70179
N. halobia DSM 20541
N. sp. F
N. sp. GY074
N. sp. GY239
N. sp. M8
N. lutea YIM 70081
N. sandarakina CG 35
N. jeotgali CD08 7
N. aurantiaca CK5
N. aurantiaca DSM 27373
N. sp. AN1
N. jeotgali strain JG-241
N. sp Act20
N. sandarakina YIM 70009
N. halotolerans YIM70084
Kocuria rhizophila TA68
B
N. aurantiaca DSM 27373
N. sp. AN1
N. sp Act20
N. jeotgali CD08 7
N. sandarakina CG 35
N. alba DSM 19423
N. sp. RB2
N. sp. GY239
N. sp. JCM 19054
N. massiliensis NP1
N. sp. M8
N. sp. PF2B19
N. sp. F
N. sp. NBAIMH1
N. sp. GY074
N. sp. populi DSM27959
Percentage Identity
100
95
90
85

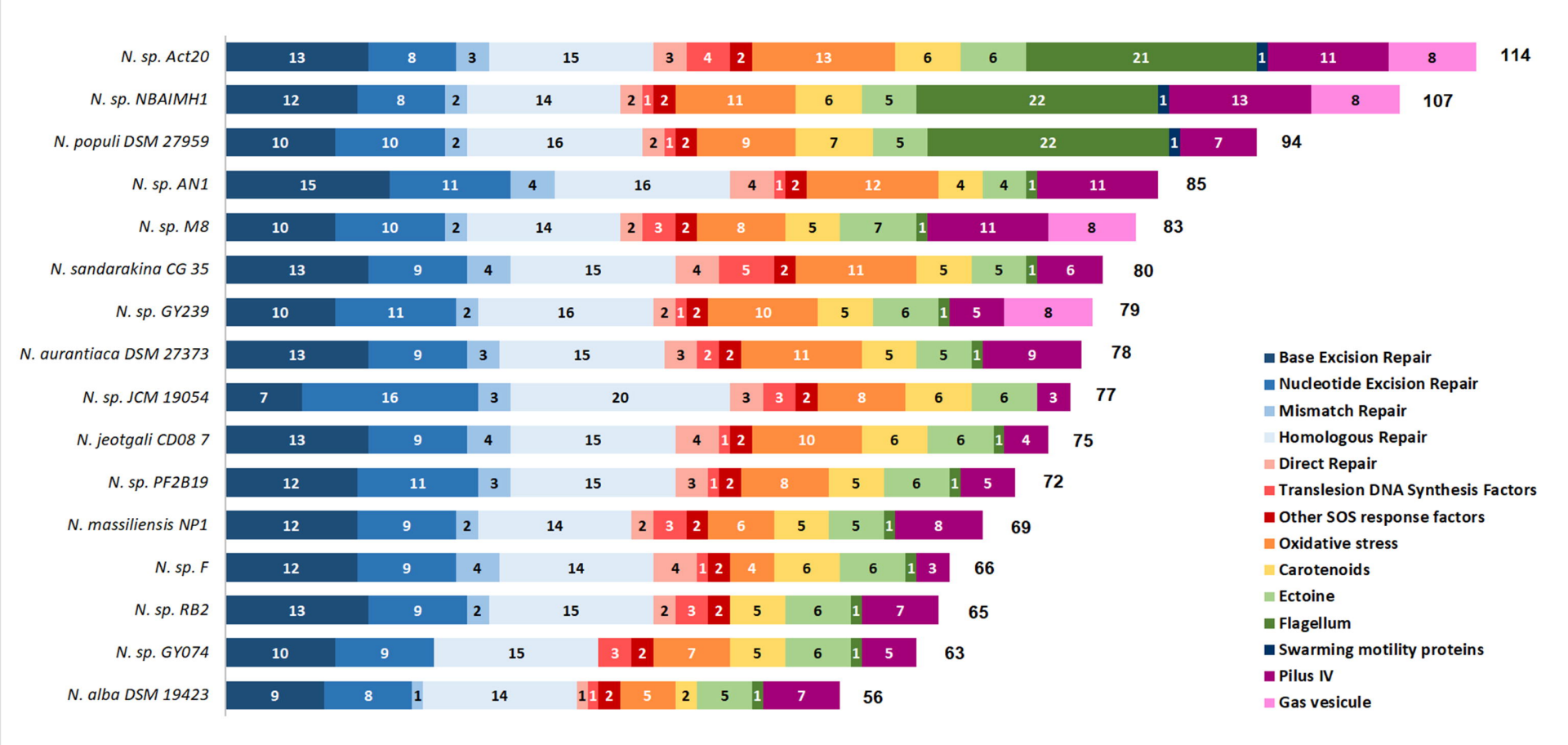
N. sp. Act20
13 8 3 15 3 4 2 13 6 6 21 1 11 8
114
N. sp. NBAIMH1
12 8 2 14 2 1 2 11 6 5 22 1 13 8
107
N. populi DSM 27959
10 10 2 16 2 1 2 9 7 5 22 1 7
94
N. sp. AN1
15 11 4 16 4 1 2 12 4 4 1 11
85
N. sp. M8
10 10 2 14 2 3 2 8 5 7 1 11 8
83
N. sandarakina CG 35
13 9 4 15 4 5 2 11 5 5 1 6
80
N. sp. GY239
10 11 2 16 2 1 2 10 5 6 1 5 8
79
N. aurantiaca DSM 27373
13 9 3 15 3 2 2 11 5 5 1 9
78
N. sp. JCM 19054
7 16 3 20 3 3 2 8 6 6 3
77
N. jeotgali CD08 7
13 9 4 15 4 1 2 10 6 6 1 4
75
N. sp. PF2B19
12 11 3 15 3 1 2 8 5 6 1 5
72
N. massiliensis NP1
12 9 2 14 2 3 2 6 5 5 1 8
69
N. sp. F
12 9 4 14 4 1 2 4 6 6 1 3
66
N. sp. RB2
13 9 2 15 2 3 2 5 6 1 7
65
N. sp. GY074
10 9 15 3 2 7 5 6 1 5
63
N. alba DSM 19423
9 8 1 14 1 1 2 5 2 5 1 7
56
Base Excision Repair
Nucleotide Excision Repair
Mismatch Repair
Homologous Repair
Direct Repair
Translesion DNA Synthesis Factors
Other SOS response factors
Oxidative stress
Carotenoids
Ectoine
Flagellum
Swarming motility proteins
Pilus IV
Gas vesicule

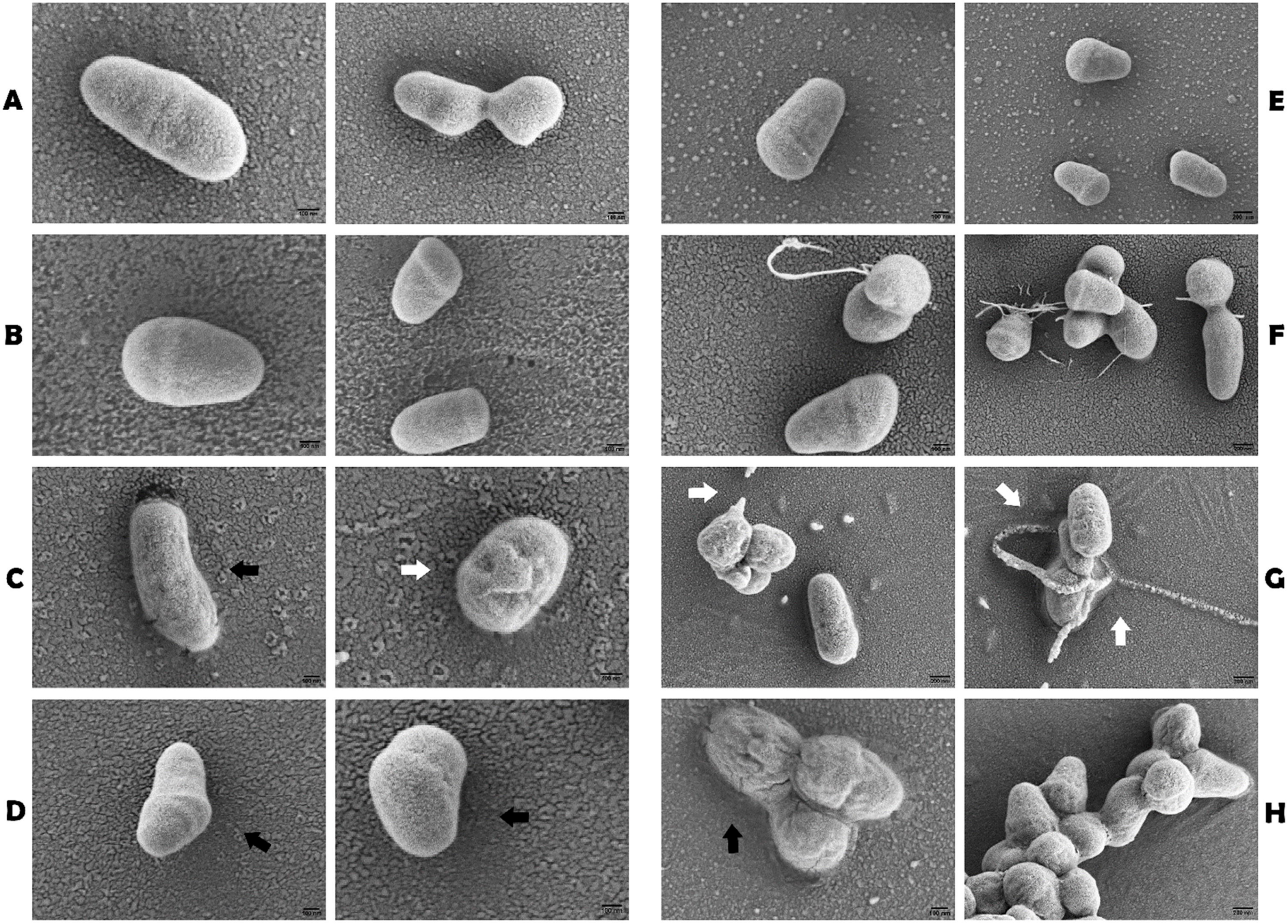
A
B
C
D
E
F
G
H

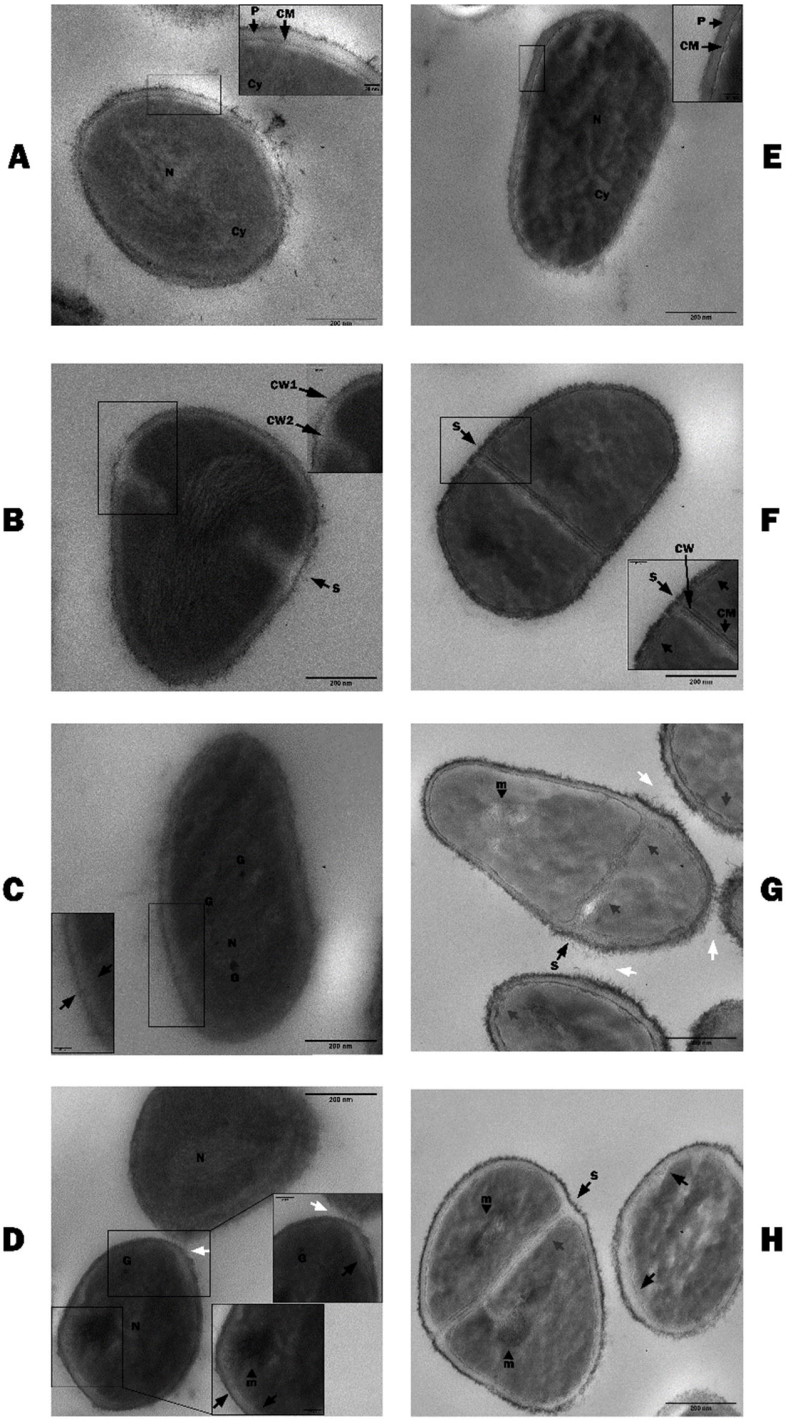
A
P
CM
Cy
N
Cy
E
P
CM
N
Cy
B
CW1
CW2
S
F
S
CW
S
CM
C
G
G
N
G
G
m
S
D
N
G
G
N
m
H
S
m
m

High UV
High arsenic content
Heavy metal content
Hypoxia
-20 °C to 20 °C
Hypersalinity
Low nutrient availability

Lake Socompa
(surrounding soil)

Martian surface

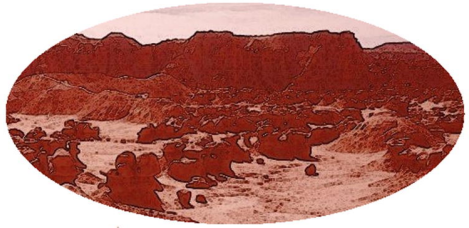

High UV
High heavy metal content
Perchlorates
Fluorine containing minerals
Hypersalinity
-140 °C to 30 °C

UV-resistome
Base Excision Repair
Nucleotide Excision Repair
Mismatch Repair
Homologous Repair
Direct Repair
Translesion DNA Synthesis Factors
Oxidative Stress
Ectoine + Carotenoids
Flagellum + Swarming Motility
Pilus IV
Gas Vesicule

Heavy metal resistance
Copper, cobalt, zinc, chromate, cadmium

Arsenic resistance
arsenate reductase
arsenate-mycothiol transferase
arsenic transporter

Fluoride resistance
Resistance protein CrcB

Osmoprotection
Specific ABC transporters
Synthesis of osmoprotectans
Trehalase degradation

Nutrient starvation resistance
Phosphate and Phosphonate ABC transporters
Phosphate limitation Two-Component System
Phosphate starvation inducible proteins PhoH and SphX
Carbon starvation protein CstA

Oxygen uptake optimization
Hemoglobin

Cold resistance
Cold-shock proteins

Perchlorate respiration ?
Chlorite dismutase

Early Earth

High UV
Low nutrient availability
Arsenic cycling in oceans ? Sforma *et al.* 2014
Oxygen gradually increasing during proterozoic